

Development and Prototyping of a Capacitive Oil Level Sensor for Aeronautical Applications

Francesco Adamo, Filippo Attivissimo, Sergio de Gioia, Attilio Di Nisio, Daniel Lotano, Mario Savino

Department of Electrical and Information Engineering, Polytechnic University of Bari, Via E. Orabona 4, Bari

Abstract – Capacitive Level Sensors (CLSs) are one of the most used level-sensing technologies in the industry as they are cheap, reliable and show high sensitivity. A typical capacitive level sensor with concentric and closed cylindrical armatures has slow dynamical response when used for high viscosity liquids such as lubricating oil for aeronautic applications. This work investigates a conditioning circuit that uses a capacitance to frequency converter and that could provide fast and accurate measurements when paired with cylindrical sensor using an LC tank-based oscillator as the exciting source. The preliminary experimental results show a linear response with small error and standard deviation.

I. INTRODUCTION

Capacitive sensors are widely used in the industry for measuring several parameters in different applications, such as displacements, forces, ECG (Electrocardiogram) Signals, liquid level, and sound pressure [1]-[6]. Aircrafts require reliable level monitoring for lubricant liquids. One method for level sensing is using time domain reflectometry or microwaves [7]-[12], but this is a very complex approach that requires high-end costly hardware. Other typical level sensing methods are floating, ultrasonic or radar and hydrostatic [13]-[14]. These methods have proven to be reliable for industry sensing or automotive applications but cannot be applied to aerospace because of EMI (Electromagnetic interferences) phenomena or vibrations.

Another challenge for aeronautical application is the develop of autonomous sensor nodes for aircraft monitoring systems exploiting energy harvesters such those based on thermoelectric generators [15] or photovoltaic modules. Indeed, aircraft pass through huge outside temperature variations providing heated cabin environments too. To make use of these temperature gradients most efficiently, additional effort to characterize such systems is required [16]–[18].

This paper investigates motor oil level monitoring using a novel capacitive sensor geometry [19], focusing on

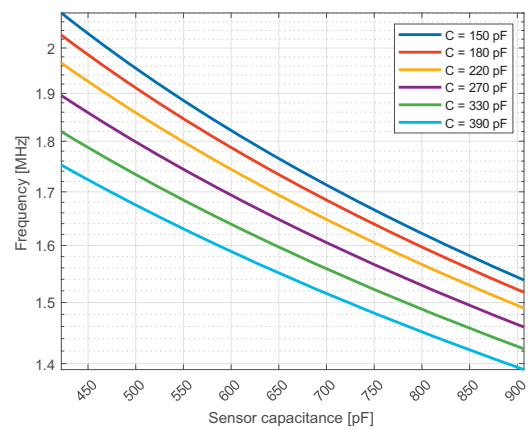


Fig. 1. Simulation of the resonant frequency of an LC tank with $L = 10 \mu\text{H}$ and $C = 150\text{-}390 \text{ pF}$ vs the sensor capacitance in parallel with C

obtaining a reduced settling time with a customized conditioning circuit. A typical capacitive level sensor is made of two concentric cylinders of conductive materials with the monitored fluid filling the intermediate gap. However, due to high lubricant oil viscosity this could result in a slow settling time of capacitance vs. time. For this reason, a different type of sensor is proposed, such as a cylindrical sensor with helical cuts on both internal and external cylinders.

Each of the cylinders is an armature of the capacitor and it is simple to calculate its capacitance when the gap between armatures is filled by the sensed medium using:

$$C_m = \frac{2\pi \cdot \epsilon_0 \cdot \epsilon_m \cdot l_m}{\ln(d_e/D_i)} \quad (1)$$

where $\epsilon_0 = 8.85 \cdot 10^{-12} \text{ F/m}$ is the vacuum dielectric constant, ϵ_m is the relative dielectric constant of the sensed liquid, l_m is its level measured from the bottom of the cylindrical sensor, d_e is the inner diameter of the external cylinder and D_i is the outer diameter of the internal cylinder.

Starting from (1) it is then possible to calculate the total capacitance of the cylindrical sensor with respect to air as

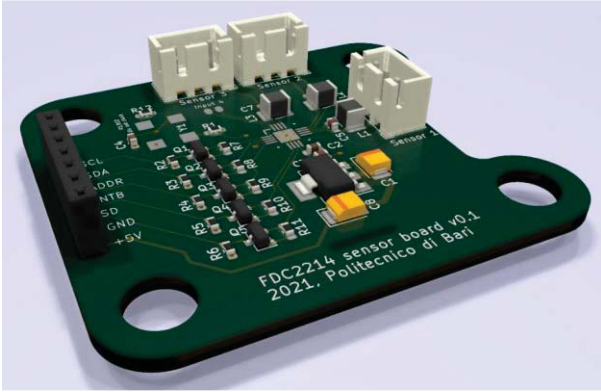


Fig. 2. Prototype rendering.

$$C_{cyl} = \frac{C_{air}}{l} (\epsilon_{air} \cdot (l - x) + \epsilon_m \cdot x) \quad (2)$$

with l being the total length of the sensor and x being the level of the sensed liquid.

Differentiating (2) with respect to x , we can obtain the sensitivity of the sensor as:

$$S = \frac{dC(x)}{dx} = \frac{C_{air}}{l} (\epsilon_m - 1). \quad (3)$$

It can be shown that the sensitivity of the cylindrical sensor is high.

As previously said, the dynamic response of the “classic” cylindrical armatures level sensor is slow. This is since there are no apertures in the cylindrical armatures, so the oil must diffuse into the gap between the armatures which is of the order of 1 mm or less. Helical cuts provide a way for the liquid to diffuse between the armatures more rapidly, making the settling time faster. The negative aspect of making helical cuts is that the mechanical structure is weaker, making the sensor more exposed to vibrations that can result in increased errors in the measure; it is then important to read the sensor with a conditioning circuit that provides high sample rates and high precision.

One of the most common, easy and cheap ways to condition a capacitive sensor is to calculate the time constant of a RC circuit [20], where the capacitance is the sensor itself or a parallel or series combination of the sensor with a fixed, reference capacitance. In fact, applying a constant voltage V to an RC circuit, the current will be given by

$$i(t) = \frac{V}{R} e^{-\frac{t}{\tau}} \quad (4)$$

where $\tau = RC$ is the time constant. Using (4) the capacitance can be calculated measuring the Δt needed to charge the capacitor to a known voltage value; the most common way to do this is using an ADC (Analog to Digital

Converter) integrated in a microcontroller.

Although the above method is easy to implement, it is highly dependent on the ADC resolution, typically limited to 12 bits or less.

For this reason, in this paper a different approach is investigated.

II. CONDITIONING CIRCUIT

A. Capacitive sensor

The conditioning circuit had to be designed to fit the initial helical capacitive sensor design, having a capacitance ranging from 422 pF to 907 pF when sensing avionic motor oil ($\epsilon_{oil} \approx 2.15$).

B. LC oscillator

A method to calculate the capacitance of a capacitive sensor is to measure the oscillating frequency of a resonant LC circuit which is a function of the capacitance. A LC tank oscillator [21] will have a well-known resonant frequency where the capacitor reactance matches the inductor reactance:

$$X_C = \frac{1}{2\pi f C} = 2\pi f L = X_L \quad (5)$$

This results in the resonant frequency

$$f = \frac{1}{2\pi \sqrt{LC_{tot}}} \quad (6)$$

In (6), C_{tot} is the total capacitance of the LC tank i.e., the sum of a fixed reference capacitor in parallel with the sensor and the parasitic capacitances (C_x and C_{par} respectively), so it can be rewritten as

$$f(C_x) = \frac{1}{2\pi \sqrt{L(C + C_{par} + C_x)}} \quad (7)$$

A variation in the sensor capacitance will result in a shift of the resonant frequency. It is easy to verify that the sensor's capacitance can be obtained as

$$C_x(f) = \frac{1}{L(2\pi f)^2} - (C + C_{par}). \quad (8)$$

C. Conditioning circuit design

The LC tank oscillator circuit was implemented using standard commercial capacitors and inductors, and the shift in the frequency was simulated in MATLAB.

The simulation was performed using a value of 10 μ H for the inductor and assuming 10 pF of parasitic capacitance. Capacitance values ranging from 150 pF to 390 pF were tested for C (Fig. 1). The chosen capacitance value was then $C = 270$ pF which would give a total frequency shift of 436.54 kHz on the full-scale range of the sensor.

The oscillation frequency is measured using a FDC2214,

that is an integrated capacitance to frequency converter IC by Texas Instruments. The FDC2214 was chosen because it has a nominal full-scale range up to 250 nF, has 4 input channels, a nominal resolution of 28 bits, an RMS noise of 0.3 fF and an output rate up to 4.08 ksamples/s. It is also easy to interface to a microcontroller thanks to its I²C (Inter Integrated Circuit) interface.

D. Prototype

Fig. 2 shows the render of the conditioning circuit prototype; the PCB (Printed Circuit Board) was designed using the KiCad® EDA (Electronic Design Automation) software. The prototype board includes the power supply regulation circuitry to power the FDC2214 with 3.3 V starting from a 2.7-6 V input voltage, and level shift converters to permit its use with different microcontrollers (with 3.3 V or 5 V logic levels).

E. Firmware

The control firmware was written for an Arduino Uno microcontroller development system. A C++ library contains the definition of the class FDC with all the properties and methods needed for the setup and the data sampling. Speaking about the sampling methods, the user can choose to get a single sample raw data for the post processing using another software, or to get frequency or capacitance conversions directly from the library. Several measurements routines have been implemented in a FSM (Finite State Machine) taking advantage of hardware peripherals of the Atmega328P microcontroller on the Arduino Uno (e.g. low level timer control for driving the stepper without blocking measurement routines).

III. TEST RESULTS

Tests were performed using avionic kerosene ($\epsilon_{ker} \approx 1.95$) and a sensor made of carbon fiber pipes ($D_i = 20.0$ mm, $d_e = 22.0$ mm) shown in Fig. 4. For every step of level measurements, 1000 data samples were taken for the post-processing.

A first calibration process was performed with no sensor connected to the circuit. Such value was assumed as the parasitic capacitance on the PCB ($C_{par} = 12.387$ pF) that is close to the estimated value of 10 pF. This value is used in (8) to get the sensor's capacitance.

The increase of the liquid level was simulated using a stepper motor driving a T6 lead screw with 1 mm pitch, such that for every 250 steps of the motor a container full of kerosene would move upwards exactly 1.25 mm for a total of 75 mm during the whole experiment. The sensor was held in position by a tripod in order to avoid any sensor's motion. A total of 61 sampling steps were made. Every sample acquisition requires 20 ms, so a single step of 1000 samples lasted 20 s.

Fig. 3 shows in red the sampled data. The first sample

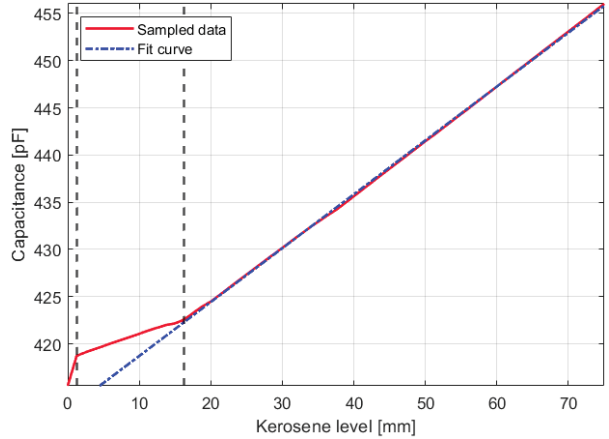


Fig. 3. Linear fitting of the sampled data; fit only considers levels above 16.25 mm

reports the sensor barely touching the liquid (415.6 pF). The second sample, when the fuel tank moves 1.25 mm upwards, has the sensor touching the liquid (418.7 pF). It is necessary to notice that the two concentric pipes are held in fixed relative position by 3 spacers made of electrical adhesive tape, thus having less air gap for the oil. For this reason, the samples up to 16.25 mm show a lower sensitivity. It is still noticeable that the lower part of the sensor is still linear.

Samples obtained for kerosene levels > 16.25 mm show a linear distribution. Data fitting was done using a first-grade polynomial expressed as

$$C_{fit} = p_1 \cdot h + p_2 \quad (9)$$

with $p_1 = 0.5707$ pF/mm and $p_2 = 413$ pF.

The residuals are calculated as

$$r_i = C_{sampled} - C_{fit} \quad (10)$$

The residuals have been plotted in Fig. 5. The root mean square error is $RMSE = 0.1229$ pF and the mean standard deviation of the steps is $\sigma = 124.2$ fF to provide uncertainty estimation and evaluate repeatability of the measurement method [22].

To evaluate the effect of the number of samples of each step, data were decimated: using the first 10 samples of the same dataset resulted in a new $RMSE = 0.1240$ pF (that is $\Delta RMSE = 0.0011$ pF) and $\sigma = 125.3$ fF (that is $\Delta\sigma = 1.1287$ fF). Hence, a difference of less than 1% was observed.

The results show a high precision and repeatability of the measurement system and the model in (9) proves that there is a sensitivity of 570.7 fF/mm.

The difference in standard deviations shows that 10 samples are enough for an accurate measure, that requires 200 ms.

Further improvements can be done on the system if a trade-off with the precision is acceptable.



Fig. 4. Carbon fiber sensor rendering (left) and dimensions (right)

CONCLUSIONS

In this paper the authors have presented a linear and high sensitivity capacitive level sensor able to measure oil level for aerospace industry. The preliminary test results obtained by the presented experimental setup has produced results in good agreement with theoretical analysis. Further investigation will be done to validate the proposed prototype and to verify repeatability and reproducibility of the system.

IV. APPENDIX: RELATIVE ERROR TO PERMITTIVITY CHANGES

A change in permittivity causes a variation in the value of the liquid level corresponding to a given measured capacitance which can be calculated with first order approximation as follows. Starting from the formula of the capacitance C as a function of the level x relative to the bottom end of the sensor:

$$C(x) = C_0 [(\varepsilon_{l,r} - 1) \frac{x}{L} + 1] \quad (11)$$

where C_0 is the capacitance of the empty sensor and L is its length, the functional dependence of x from the relative permittivity $\varepsilon_{l,r}$ is obtained by inversion of (11):

$$x(\varepsilon_{l,r}) = \frac{C/C_0 - 1}{\varepsilon_{l,r} - 1} L \quad (12)$$

Then, if the relative permittivity of the liquid is changed from $\varepsilon_{l,r}$ to $\varepsilon'_{l,r} = \varepsilon_{l,r} + \Delta\varepsilon_{l,r}$ the level at which a given capacitance value C is measured can be obtained expanding (12) with a Taylor series:

$$x(\varepsilon'_{l,r}) = x(\varepsilon_{l,r}) - \frac{C/C_0 - 1}{(\varepsilon_{l,r} - 1)^2} L (\varepsilon'_{l,r} - \varepsilon_{l,r}) + \text{higher order terms} \quad (13)$$

Then putting (12) into (13), the relative variation of the level with respect to the relative variation of the relative permittivity at any value of the measured capacitance is:

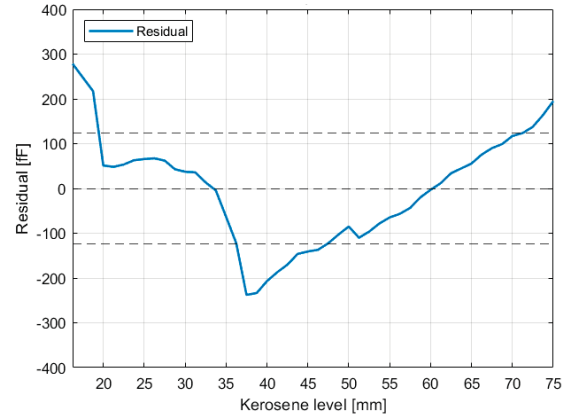


Fig. 5. Residual errors in the linear fitting of experimental data

$$\frac{\Delta x}{x} \cong - \frac{\varepsilon_{l,r}}{\varepsilon_{l,r} - 1} \frac{\Delta \varepsilon_{l,r}}{\varepsilon_{l,r}} \cong -2.05 \frac{\Delta \varepsilon_{l,r}}{\varepsilon_{l,r}} \quad (14)$$

where in the right-hand side coefficient 2.05 has been calculated for the nominal value $\varepsilon_{l,r}$ of kerosene equal to 1.95. That is, in relative terms, an increase in $\varepsilon_{l,r}$ is almost doubled to give the decrease in liquid level at any fixed value of the measured capacitance.

On the contrary, a sensor calibrated for a liquid with relative permittivity $\varepsilon_{l,r}$, if used with a liquid of a different permittivity, gives rise to a level relative error of +1.9 the relative variation of $\varepsilon_{l,r}$.

Funding: This research was funded by the MUR on the ‘‘PON R&I 2014-2020 – Area di specializzazione ‘‘Aerospazio’’, Project ‘‘FURTHER’’ with Avio Aero SpA.

ACKNOWLEDGMENTS

The authors would like to thank Dr. Giuseppe Giliberti for his valuable cooperation and consistent support.

REFERENCES

- [1] X. X. Liu, K. Peng, Z. Chen, H. Pu and Z. Yu, ‘‘A New Capacitive Displacement Sensor with Nanometer Accuracy and Long Range’’, IEEE Sensors Journal, vol. 16, no. 8, pp. 2306-2316, Apr. 2016.
- [2] M.-Y. Cheng, C.-L. Lin, Y.-T. Lai and Y. J. Yang, ‘‘A Polymer-Based Capacitive Sensing Array for Normal and Shear Force Measurement’’, Sensors, vol. 10, no. 11, pp. 10211-10225, 2010.
- [3] A. Ueno, Y. Akabane, T. Kato, H. Hoshino, S. Kataoka and Y. Ishiyama, ‘‘Capacitive Sensing of Electrocardiographic Potential Through Cloth from the Dorsal Surface of the Body in a Supine Position: A Preliminary Study’’, IEEE Transactions on Biomedical Engineering, vol. 54, no. 4, pp. 759-766, Apr. 2007.
- [4] Ragolia, M.A.; Lanzolla, A.M.L.; Percoco, G.;

- Stano, G.; Di Nisio, A. Thermal Characterization of New 3D-Printed Bendable, Coplanar Capacitive Sensors. *Sensors* 2021, 21, 6324. doi: 10.3390/s21196324
- [5] Yang, Q.; Yu, A.J.; Simonton, J.; Yang, G.; Dohrmann, Y.; Kang, Z.; Li, Y.; Mo, J.; Zhang, F.-Y. An inkjet-printed capacitive sensor for water level or quality monitoring: Investigated theoretically and experimentally. *J. Mater. Chem. A* 2017, 5, 17841–17847
- [6] R. N. Miles, W. Cui, Q. T. Su and D. Homencovschi, "A MEMS Low-Noise Sound Pressure Gradient Microphone with Capacitive Sensing", *Journal of Microelectromechanical Systems*, vol. 24, no. 1, pp. 241-248, Feb. 2015.
- [7] M. Scarpetta, M. Spadavecchia, F. Adamo, M.A. Ragolia and N. Giaquinto, "Detection and Characterization of Multiple Discontinuities in Cables with Time-Domain Reflectometry and Convolutional Neural Networks." *Sensors* 2021, 21, 8032. <https://doi.org/10.3390/s21238032>
- [8] M. Scarpetta, M. Spadavecchia, G. Andria, M. A. Ragolia and N. Giaquinto, "Analysis of TDR Signals with Convolutional Neural Networks," 2021 IEEE International Instrumentation and Measurement Technology Conference (I2MTC), 2021, p.1-6, doi: 10.1109/I2MTC50364.2021.9460009.
- [9] M. Vogt, C. Schulz, C. Dahl, I. Rolfes and M. Gerding, "An 80 GHz radar level measurement system with dielectric lens antenna," 2015 16th International Radar Symposium (IRS), 2015, pp. 712-717, doi: 10.1109/IRS.2015.7226222.
- [10] Kunde Santhosh Kumar, A. Bavithra, M. Ganesh Madhan, "A cavity model microwave patch antenna for lubricating oil sensor applications," *Materials Today: Proceedings*, 2022, doi: 10.1016/j.matpr.2022.06.136.
- [11] A.M. Loconsole, V.V. Francione, V. Portosi, O. Losito, M. Catalano, A. Di Nisio, F. Attivissimo, F. Prudeniano, "Substrate-Integrated Waveguide Microwave Sensor for Water-in-Diesel Fuel Applications," *Appl. Sci.* 2021, vol. 11, no. 21, art. no. 10454, Nov. 2021, doi: 10.3390/app112110454
- [12] G. Andria, F. Filippo Attivissimo, S.M. Camporeale, A. Di Nisio, P. Pappalardi, A. Trotta, "Design of a Microwave Sensor for Measurement of Water in Fuel Contamination," *Measurement*, vol. 136, Mar. 2019, pp. 74-81, doi: 10.1016/j.measurement.2018.12.076.
- [13] J. Kredba and M. Holanda, «Precision ultrasonic range sensor using one piezoelectric transducer with impedance matching and digital signal processing,» 2017 IEEE International Workshop of Electronics, Control, Measurement, Signals and their Application to Mechatronics (ECMSM), pp. 1-6.
- [14] J. Huang, Z. Zhou, X. Wen and D. Zhang, «A diaphragm-type fiber Bragg grating pressure sensor with temperature compensation,» *Measurement*, p. 1041–1046, 2013.
- [15] D. Samson, T. Otterpohl, M. Kluge, U. Schmid, e Th. Becker, "Aircraft-Specific Thermoelectric Generator Module", *Journal of Electronic Materials*, vol. 39, n. 9, p. 2092–2095, set. 2010, doi: 10.1007/s11664-009-0997-7
- [16] F. Attivissimo, C. Guarnieri Calò Carducci, A.M.L. Lanzolla, M Spadavecchia. "An extensive unified thermo-electric module characterization method", *Sensors*, vol. 16, no. 12, pp. 1-20
- [17] C. Guarnieri Calò Carducci, M. Spadavecchia, e F. Attivissimo, «High accuracy testbed for thermoelectric module characterization», *Energy Conversion and Management*, vol. 223, 2020, doi: 10.1016/j.enconman.2020.113325.
- [18] F. Adamo, F. Attivissimo, A. Di Nisio, e M. Spadavecchia, "Analysis of the Uncertainty of the Double-diode Model of a Photovoltaic Panel", in 2011 IEEE International Instrumentation & Measurement Technology Conference Proceedings, 2011, p.616–620. doi: 10.1109/IMTC.2011.5944253.
- [19] L. De Palma, F. Adamo, F. Attivissimo, S. de Gioia, A. Di Nisio, A. M. L. Lanzolla and M. Scarpetta, "Low-cost capacitive sensor for oil-level monitoring in aircraft," 2022 IEEE International Instrumentation and Measurement Technology Conference (I2MTC), 2022, pp. 1-4, doi: 10.1109/I2MTC48687.2022.9806667.
- [20] W. Djatmiko, "Capacitance Measurements System Using RC Circuit", *Social Sciences*, vol. 3, no. 12, pp. 603-610, Mar. 2019.
- [21] B. V. Rao, "Electronic Circuit Analysis", Pearson Education India, 2011.
- [22] F. Attivissimo, A. Cataldo, L. Fabbiano, N. Giaquinto, "Systematic errors and measurement uncertainty: An experimental approach", *Measurement*, vol. 44, no. 9, pp. 1781-1789, Nov. 2011